

In-situ growth of Copper oxide on MXene by combustion method for electrochemical ammonia production from nitrate ion

Sagar Ingavale¹, Phiralang Marbaniang², Manoj Palabathuni¹ and Nimai Mishra³

¹*Department of Chemistry, SRM University-AP, Andhra Pradesh, Neerukonda, Guntur (Dt), Andhra Pradesh, India 522240.*

²*Department of Chemistry, Indian Institute of Technology Madras, Chennai-600036, India*

³*Institute of Chemical Technology Mumbai, IOC Odisha Campus Bhubaneswar, Bhubaneswar, Odisha, India 751013*

2. Materials and Methods

2.1 Materials

MAX phase purchased from MAX phase and MXene Ceramic Technology, China. Nafion and $\text{Cu}(\text{NO}_3)_2 \cdot 6\text{H}_2\text{O}$ were purchased from Sigma-Aldrich. Ammonium chloride (99.5%), sodium nitroferrocyanide(III)dihydrate (99%), K_2SO_4 , KNO_3 , Hydrazine monohydrate (98%), 4-(Dimethylamino) benzaldehyde (99%) were purchased from Sigma. Sodium hypochlorite Pentahydrate purchased from TCI. Salicylic acid received from Thermo Fisher. All chemicals are purchased as an analytical grade and were used without being tested for purity.

Physical Characterization:

X ray powder diffraction (XRD) measurements were analysed on X'pert pro diffractometer, PANalytical using CuK_α line ($\lambda = 1.54 \text{ \AA}$, 40 kV, 40 mA) in the 2θ range of 5° to 80° with scan rate $2^\circ/\text{min}$. The morphology of the optimized samples were studied by using 'Quanta 200 FEG FE SEM'. High-resolution Transmission electron microscopy (TEM) analysis carried out by using a JEOL Japan, JEM 2100 Plus microscope operated at 100 kV. X ray photoelectron spectroscopy (XPS) performed by using Shimadzu ESCA 3400 instrument using $\text{AlK}\alpha$ source (Physical Electronics system; 1486.6 eV monochromatic beam) operated at 15 kV and the XPSPEAK41 software was used for curve fitting and data analysis. Linear type background was used for data processing.

Electrochemical Measurements:

The electrochemical analysis was carried out by using biologic instruments. The H-type of electrochemical cells (H-cell) with two compartments separated by porous frit was used for electrochemical measurements. Here, three electrode system was employed in which counter electrode was placed in another compartment of H-cell and working and reference electrode was placed in same compartment. The working electrode was prepared by using catalyst coated on carbon paper. At first, 6 mg of catalyst was dispersed in 1 ml solution of 796 μL de-ionized water, 200 μL isopropanol and 4 μL Nafion (5 wt% Sigma-Aldrich). Further, the vertex vibrator used to form homogenous ink solution for five minutes. Then, 20 μL of catalysts solution was drop casted on the surface of carbon paper. Further allowed it for four hours to dry at room temperature. The loading of active electro-catalysts on the carbon paper was approximately 0.12 mg cm^{-2} . Platinum wire and Ag/AgCl (saturated KCl) were used as a counter and reference electrode respectively. At last, the potentials were converted with respect to RHE by using $E_{\text{RHE}} = E_{\text{Ag/AgCl}} + 0.198 \text{ V} + 0.0591 \text{ pH}$. Here, 0.1 M K_2SO_4 solution containing 0.5 M KNO_3 was used as an electrolyte. The electrochemical nitrate reduction to form ammonia was carried out by using linear sweep voltammetry (LSV) and chronoamperometric techniques. The LSV was analysed from -0.9 to 0v vs RHE at scan rate 10 mV/s. Chronoamperometric measurements performed at various potential for half an hour.

Determination of ion concentration:

The ultraviolet-visible (UV-Vis) spectrophotometer was used to the ammonia and hydrazine detection after electrochemical nitrate reduction after diluting to appropriate concentration to match the range of calibration curves. The concentration of NH_3 and hydrazine ions were measured with respect to the corresponding standard calibration curve by analyzing standard solution. The respective detection methods are as follow:

Ammonia Quantification

Indophenol blue technique is widely used for ammonia detection and estimation. Initially, the standardization of ammonia was carried out with respect to know concentration of ammonium chloride solution. The standard solution of ammonium chloride prepared in 0.1 M K_2SO_4 since it

used as an electrolyte. The solution for measurement was prepared by mixing 2 ml of standard ammonia chloride solution, 2 ml of a 1 M NaOH solution containing 5 wt % salicylic acid + 5 wt % sodium citrate, 1 ml of 0.05 M NaClO and 0.2 ml of 1.0 wt % $C_5FeN_6Na_2O$. Subsequently, the solution lightly shaken for 30 seconds and kept undisturbed for 2 h at room temperature. Finally, the absorbance of these various solutions was measured at 650 nm by using UV-Vis spectrometer to obtain standard calibration curve of ammonia solution. By following a similar method, the ammonia quantification from electrolyte solution was measured.

Hydrazine quantification

UV-Vis spectrometer used for determining hydrazine concentration. At first, standard hydrazine solution was used for the standardization of hydrazine. In short, the 0, 0.5, 1, 1.5, 2, 2.5, 3 $\mu\text{g/ml}$ of hydrazine solutions were synthesized in 0.1 M K_2SO_4 . Further, 2 ml of standard colouring solution (0.599 g of para-(dimethylamino) Benzaldehyde dissolved in solution containing 3 ml concentrated HCl in 30 ml ethanol) was added to the 2 ml of standard hydrazine solutions and shaken for 30 seconds. After, the solutions were kept undisturbed for 15 minutes. Finally, the absorbance was measured at from 400 to 500 nm by using a UV-Vis spectrometer.

The Faradaic Efficiency and NH_3 Yield:

Faradic efficiency and ammonia yield was calculated by using the chronoamperometric analysis followed by the UV-Vis spectrophotometer. The chronoamperometric analysis was done at various potentials for half an hour. The Faradaic efficiency (FE) of ammonia (NH_3) was calculated as follows:

$$FE_{\text{ammonia}} = (8 \times F \times C_{\text{ammonia}} \times V / 17 \times Q) \times 100\%$$

where F, C_{ammonia} , V, and Q refer to the Faraday constant (96485 C mol^{-1}), measured NH_3 concentration, volume of the cathodic electrolyte, and the total charge passing the cell, respectively.

The yield of ammonia:

$$\text{Yield}_{\text{ammonia}} = c_{\text{ammonia}} \times V / (t \times m)$$

Where, c , V , t and m represents concentration of ammonia, volume of electrolyte, electrolysis time and loading of catalyst respectively.

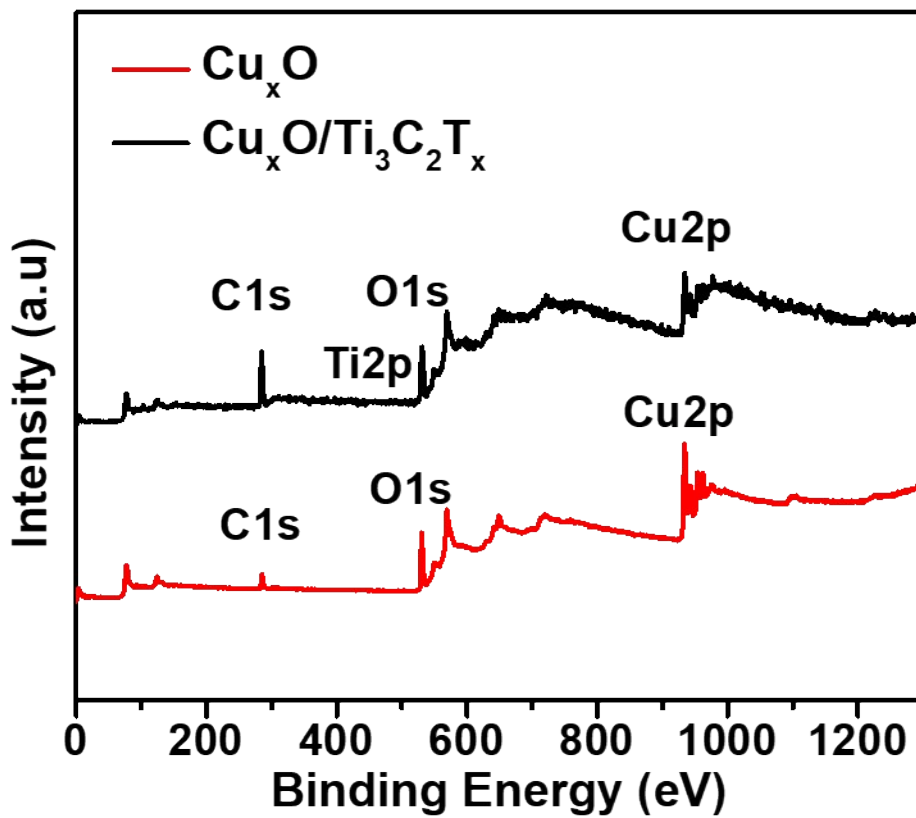


Figure S1: XPS Survey spectra for Cu_xO and $\text{Cu}_x\text{O}/\text{Ti}_3\text{C}_2\text{T}_x$

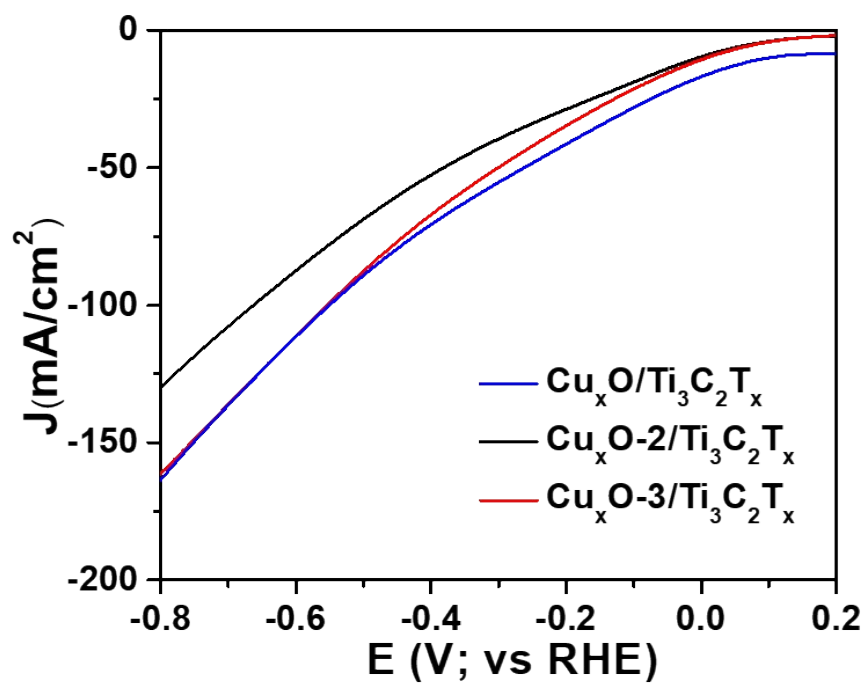


Figure S2: (a) LSVs curve for $\text{Cu}_x\text{O}/\text{Ti}_3\text{C}_2\text{T}_x$, $\text{Cu}_x\text{O-2}/\text{Ti}_3\text{C}_2\text{T}_x$ and $\text{Cu}_x\text{O-3}/\text{Ti}_3\text{C}_2\text{T}_x$ at 10 mV s^{-1} with nitrate ions in $0.1 \text{ M K}_2\text{SO}_4$ electrolyte

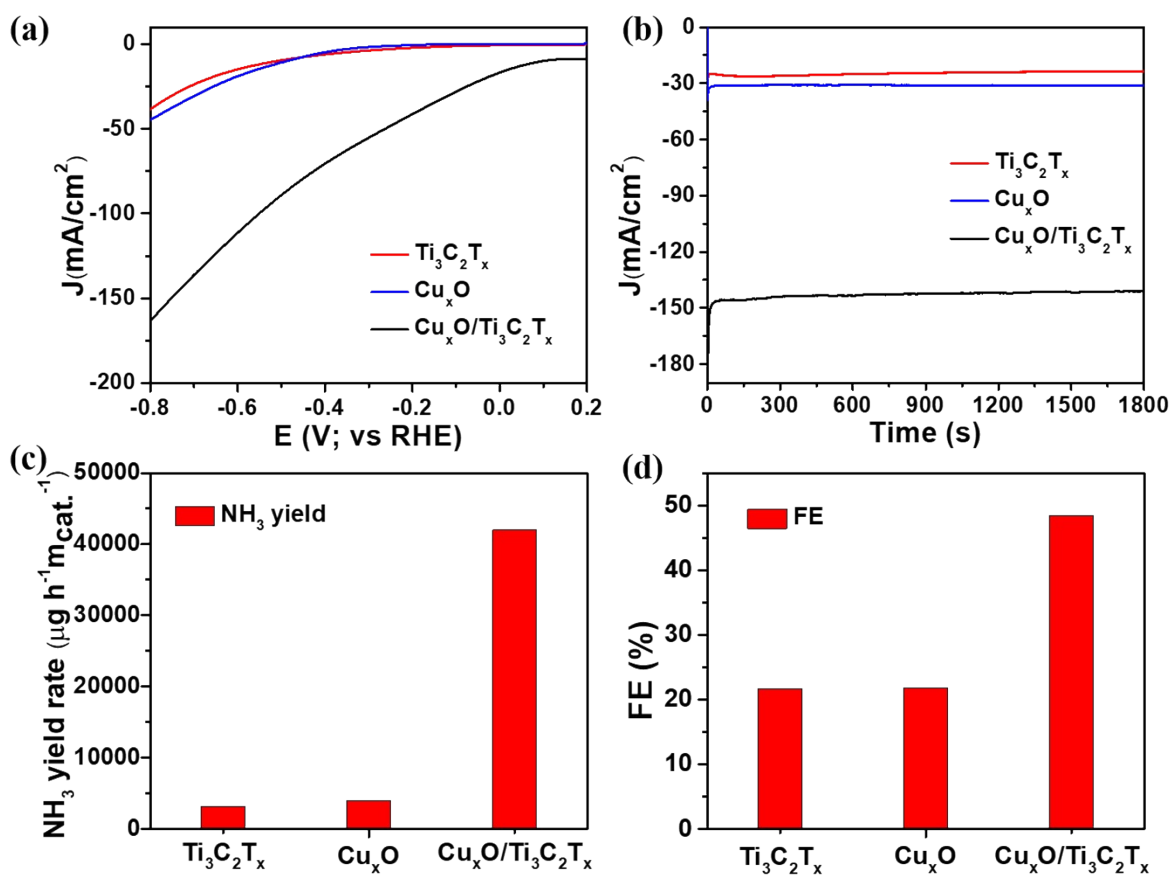


Figure S3: (a) Comparative LSV pattern at 10 mV s^{-1} and (b) chronoamperometric curve of $\text{Cu}_x\text{O}/\text{Ti}_3\text{C}_2\text{T}_x$, Cu_xO and $\text{Ti}_3\text{C}_2\text{T}_x$ with nitrate ions in $0.1 \text{ M K}_2\text{SO}_4$ electrolyte. (c) NH_3 yield and (d) Faradaic efficiency for NH_3 production of $\text{Ti}_3\text{C}_2\text{T}_x$, Cu_xO and $\text{Cu}_x\text{O}/\text{Ti}_3\text{C}_2\text{T}_x$ catalyst at -0.7 V vs RHE.

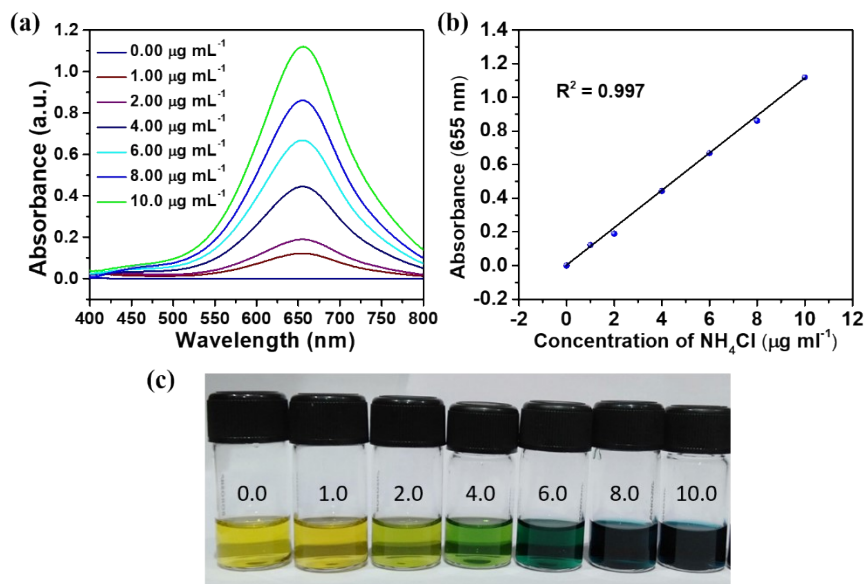


Figure S4: (a) UV-Vis spectra for indo-phenol determination of different known concentrations of NH_4^+ standards. (b) Calibration curve obtained from linear fit. (c) Photograph of standard NH_4^+ solution.

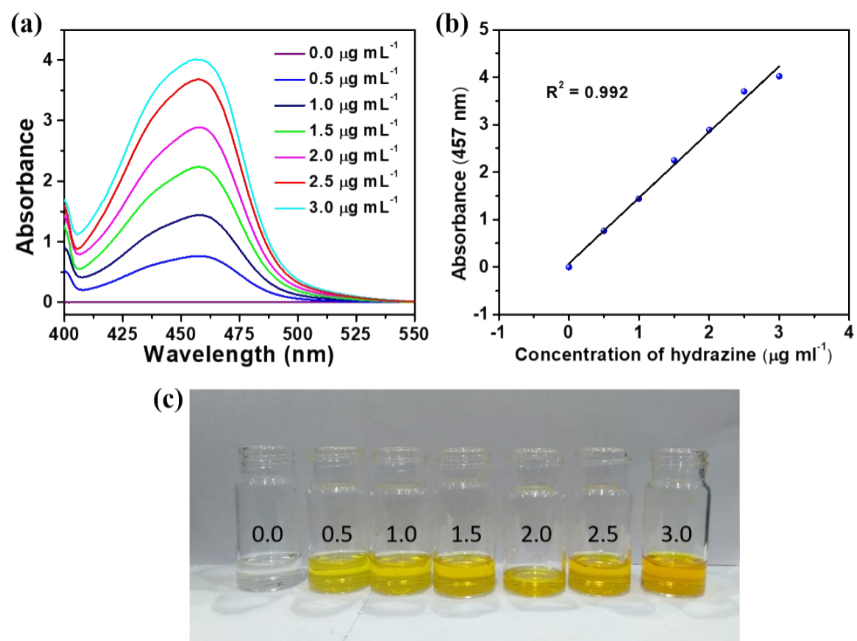


Figure S5: (a) UV-Vis spectra for Watt and Chrisp determination of different known concentrations of hydrazine standards. (b) Calibration curve obtained from linear fit. (c) Photograph of standard hydrazine solution.

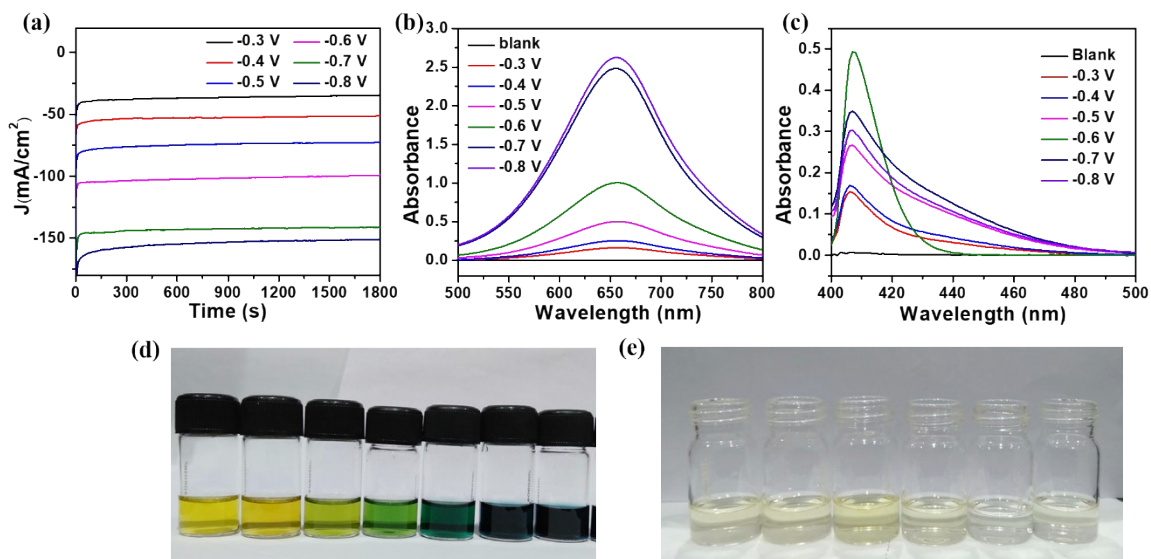


Figure S6: (a) Electrochemical i-t experiments at various applied potential of $\text{Cu}_x\text{O}/\text{Ti}_3\text{C}_2\text{T}_x$ catalyst, UV-Vis spectra for (b) indo-phenol determination of ammonia and (c) Watt and Chrisp determination of hydrazine in electrolytes obtained from electrocatalytic CA experiments at different applied potentials respectively. (d-e) Photograph of ammonia and hydrazine solution.

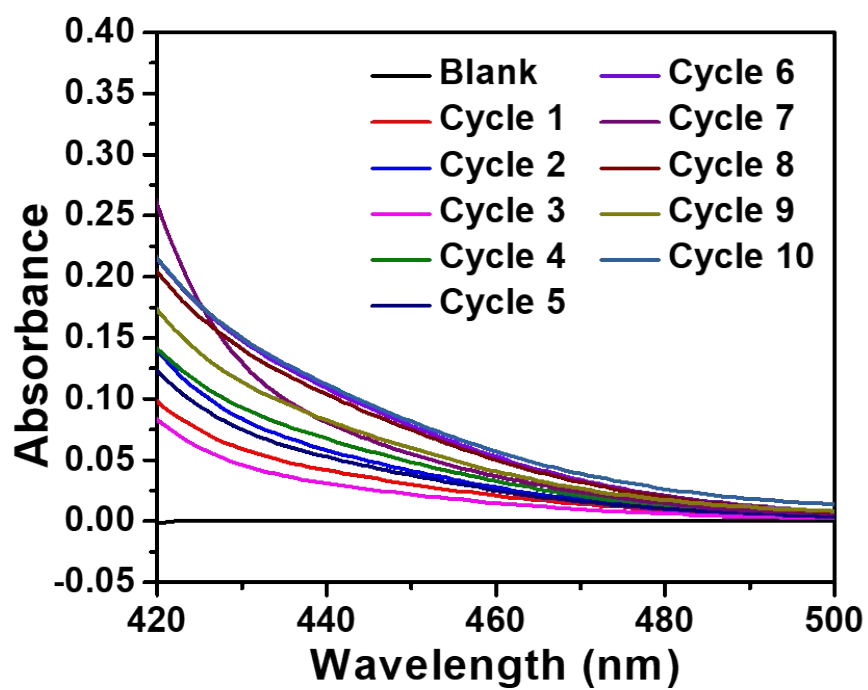


Figure S7: UV-Vis spectra for Watt and Chrisp determination of hydrazine in electrolytes obtained from electrocatalytic CA experiments at -0.7 V vs RHE.

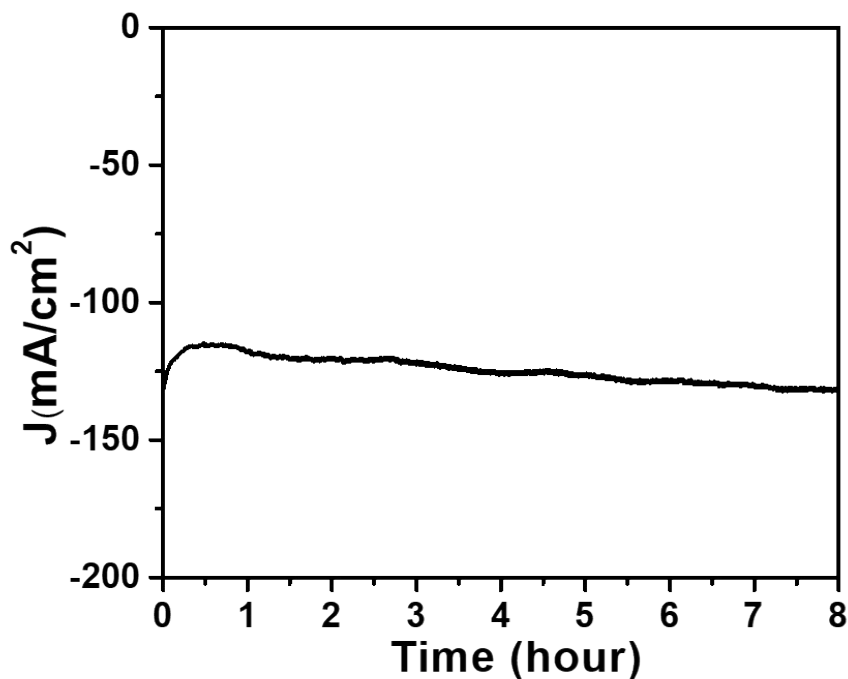


Figure S8: Chronoamperometric analysis of $\text{Cu}_x\text{O}/\text{Ti}_3\text{C}_2\text{T}_x$ catalyst at -0.7 V vs RHE in 0.5 M $\text{KNO}_3 + 0.1$ M K_2SO_4 electrolyte.

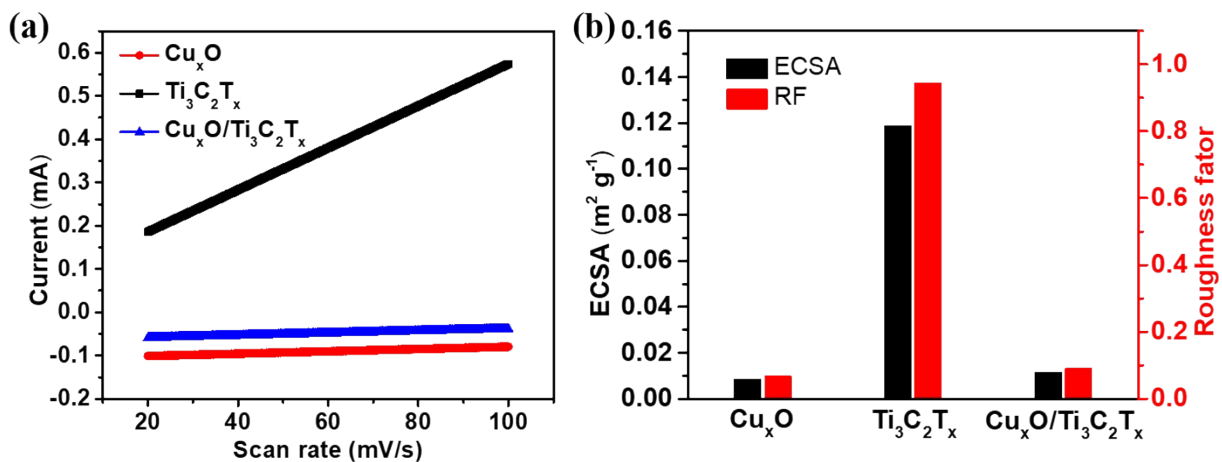


Figure S9: (a) Comparative current vs scan rate profile; (b) ECSA and roughness factor for Cu_xO , $\text{Ti}_3\text{C}_2\text{T}_x$, and $\text{Cu}_x\text{O}/\text{Ti}_3\text{C}_2\text{T}_x$ electrocatalysts.

Table S1: Comparison of electro-catalytic performance of various copper based electrocatalysts for nitrate reduction

Sr. No.	Catalysts	Overpotential	NH ₃ yield	FE [%]	Ref
1	Cu _x O/Ti ₃ C ₂ T _x	-0.7 V vs RHE	41982 μgh ⁻¹ m _{cat} ⁻¹	48	Present work
2	Cu-Sn-Bi	-1.5 vs SCE	0.005 mmol h ⁻¹ cm ⁻²	19	1
3	Cu/rGO/GP	-1.4 V vs SCE	0.014 mmol h ⁻¹ cm ⁻²	29.93	2
4	Copper electrode with fiber 1% Pd	--	0.038 mmol h ⁻¹ cm ⁻²	38	3
5	CuO x nanoparticles	--	449.41 μg h ⁻¹ mg _{cat} ⁻¹	74	4
6	Pd/C	-0.2 V vs. RHE	307 μg h ⁻¹ mg _{Pd}	35.1	5
7	oxide-derived Cu	-0.15 V vs RHE	1.1 mmol h ⁻¹ cm ⁻²	92	6
8	Au ₁ Cu(111)	-0.2 V vs RHE	555 μg h ⁻¹ cm ⁻²	98.7	7
9	CuPd nanocubes	-0.6 V vs RHE	6.25 mol h ⁻¹ mg _{cat} ⁻¹	92.5	8
10	Cu ₂ O	-1.2 V vs Ag/AgCl	0.0699 mmol h ⁻¹ mg ⁻¹	85.2	9
11	CuPc@MXene	-1.06 V vs RHE	0.27 mg h ⁻¹ cm ⁻²	94.0	10
12	Cu/CuO	-0.85 V vs RHE	0.2449 mmol h ⁻¹ cm ⁻²	95.8	11

References

- 1 W. Gao, L. Gao, J. Meng, D. Li, Y. Guan, L. Cui, X. Shen and J. Liang, *Water Science and Technology*, 2019, **79**, 198–206.
- 2 D. Yin, Y. Liu, P. Song, P. Chen, X. Liu, L. Cai and L. Zhang, *Electrochimica Acta*, 2019, **324**, 134846.
- 3 T. F. Beltrame, F. M. Zoppas, M. C. Gomes, J. Z. Ferreira, F. A. Marchesini and A. M. Bernardes, *Chemosphere*, 2021, **279**, 130832.
- 4 J. Geng, S. Ji, H. Xu, C. Zhao, S. Zhang and H. Zhang, *Inorganic Chemistry Frontiers*, 2021, **8**, 5209–5213.
- 5 J. Lim, C. Y. Liu, J. Park, Y. H. Liu, T. P. Senftle, S. W. Lee and M. C. Hatzell, *ACS*

- Catalysis*, 2021, **11**, 7568–7577.
- 6 W. Jung and Y. J. Hwang, *Materials Chemistry Frontiers*, 2021, **5**, 6803–6823.
 - 7 Z. Gong, W. Zhong, Z. He, Q. Liu, H. Chen, D. Zhou, N. Zhang, X. Kang and Y. Chen, *Applied Catalysis B: Environmental*, 2022, **305**, 121021.
 - 8 Q. Gao, H. S. Pillai, Y. Huang, S. Liu, Q. Mu, X. Han, Z. Yan, H. Zhou, Q. He, H. Xin and H. Zhu, *Nature Communications*, 2022, **13**, 1–12.
 - 9 Q. Zhao, Z. Tang, B. Chen, C. Zhu, H. Tang and G. Meng, *Chemical Communications*, 2022, **58**, 3613–3616.
 - 10 K. Li, Y. Lei, J. Liao and Y. Zhang, *Inorganic Chemistry Frontiers*, 2021, **8**, 1747–1761.
 - 11 Y. Wang, W. Zhou, R. Jia, Y. Yu and B. Zhang, *Angewandte Chemie - International Edition*, 2020, **59**, 5350–5354.